

Evaluation of Lithium-ion Batteries Following a Single Thermal Insult

Gordon H. Waller¹, Rachel E. Carter¹, Patrick J. West², Corey T. Love¹

¹Chemistry Division

²ASEE Post-doctoral Fellow

U.S. Naval Research Laboratory

Washington, DC 20375 USA

Abstract: *Lithium-ion batteries were subjected to temperatures above the manufacturer specifications in a single “thermal insult” to explore the lasting impacts of these one-time mild abuse events. After the thermal insult, galvanostatic cycling and electrochemical impedance spectroscopy were used to determine impacts on the cell capacity and impedance. Isothermal Battery Calorimetry (IBC) was used to observe changes in heat generation during cycling, while Accelerating Rate Calorimetry (ARC) was used to evaluate the thermal runaway behavior of the cells. The results in this study indicated that commercial-off-the-shelf 18650 are extremely robust to the test conditions explored in this study, and no significant impacts to cell performance or safety were observed. However, current-interrupt-device (CID) activation was observed with sufficiently high temperatures and exposure durations.*

Keywords: Lithium-ion batteries; battery safety; thermal abuse; isothermal battery calorimetry; accelerating rate calorimetry

Introduction

Lithium-ion batteries (LIB) typically have a manufacturer recommended temperature range of 0 °C to 60 °C depending on operation. Electrochemical cycling at the extreme ends of this temperature range is known to result in accelerated capacity fade and impedance rise for most LIB [1]. Heating cells well above the recommended upper temperature limit is a common method to evaluate the safety of lithium-ion batteries. Above some critical temperature, LIB undergo a series of exothermic reactions leading to rapid self-heating, referred to as thermal runaway [2]. Exothermic reactions in LIB begin with decomposition of the solid electrolyte interphase (SEI) layer on the anode at temperatures in the range of 60-80 °C, or just above the manufacturer recommended upper limit [2] [3]. However, temperatures above 120 °C are typically needed before self-heating can no longer be mitigated through passive heat rejection and cell failure occurs. Observed LIB failures depend on chemistry, cell design, and state-of-charge but can range from relatively benign such as the activation of an internal safety device or venting electrolyte vapors to highly energetic ejections of flaming debris [4]. Aging effects by cycling or storing cells near the manufacturer recommended upper temperature limit have been evaluated previously and generally result in a higher observed onset temperatures for thermal runaway due to growth of the SEI, however reported results vary with cathode chemistry [5] [6].

The implications of exposing LIBs to temperature ranges above manufacturer recommend limits but below the onset of self-sustain thermal runaway (60 °C to 120 °C) have not been broadly studied. Moreover, an important scenario to consider is a large LIB pack containing many cells wherein one or more, but not all, of the cells have undergone thermal runaway. Propagating thermal runaway can occur due to the failure of a single cell, however brief exposures of adjacent cells to temperatures well above the manufacturer recommended limit without propagating failure is also a possibility.

Experimental

High energy (3.4 Ah, 250 Wh/kg, 700 Wh/L, NCM811 cathode and graphite/silicon composite anode) 18650 LIBs were cycled to two different states of charge (SOC) of 30% and 100% before being subjected to thermal insult at temperatures of 80 °C, 90 °C and 100 °C, for durations of 20 minutes, 100 minutes, and 24 hours. Exposure duration was defined as the time above the desired exposure temperature, with a duration of 20 minutes previously reported as the time required to reach a near-equilibrium temperature condition between the surface and center of an 18650 exposed to a temperature step [7]. A thermal ramp rate of approximately 2 °C min.⁻¹ was utilized in every test. The skin-temperature and open circuit voltage (OCV) of each cell were monitored during every thermal insult test, and each test condition was repeated at least in triplicate. Prior to the thermal insult, the capacity of each cell was measured by a C/5 (680 mA) charge and discharge cycle between a voltage range of 2.5 V and 4.2 V using a Maccor battery cycler. A constant voltage hold at 4.2 V was imposed during charging until the charging current decayed to <C/20 (170 mA). After the thermal insult, cells were discharged at a rate of C/5 to determine capacity lost during thermal insult, and then cycled at a C/5 rate to evaluate impacts on capacity retention. Electrochemical impedance spectroscopy (EIS) was collected on each cell at 30% SOC and 25 °C before and after thermal insult using a potentiostat and frequency response analyzer (PARSTAT MC Multichannel Potentiostat). Impedance change was interpreted as the increase in total impedance represented by a low-frequency intercept in a Nyquist plot, occurring at approximately 1-2 Hz. Heat generated during C/5 cycling was evaluated before and after thermal insult using isothermal battery calorimetry with an isothermal temperature of 30 °C (THT IBC-C). Thermal runaway behavior of as-received and post-thermal insult cells were evaluated using accelerating rate calorimetry (THT ARC-

ES) in “heat-wait-seek” mode, using a step size of 5 °C, wait time of 5 minutes, and seek time of 20 minutes. Exothermic behavior was defined as a self-heating rate of >0.02 °C/min, while thermal runaway was defined as a self-heating rate of >5 °C/min. All ARC measurement were conducted with cells at 100% SOC except for cells in which Current Interrupt Device (CID) activation had occurred, in which cells were somewhat below 100% due to self-discharge occurring during the thermal insult experiment.

Results

An example of cell open circuit voltage (OCV) and temperature measured using a surface-mounted thermocouple during a thermal insult experiment is shown in **Figure 1**. Cell voltage (solid lines) were observed to first increase with temperature and then began decreasing for the duration of the thermal insult. Two of three cells shown in Figure 1 experienced a rapid voltage drop prior to the end of the thermal insult, which is attributed to CID activation. Exposure to 80 °C for any duration did not result in CID activation, while 2 out of 3 cells exposed to 90 °C for 24-hours experienced CID activation. Additionally, for the cells exposed to 100 °C, CID occurred in 2 out 6 cells and 3 out of 3 cells after 100 minutes and 24 hours, respectively.

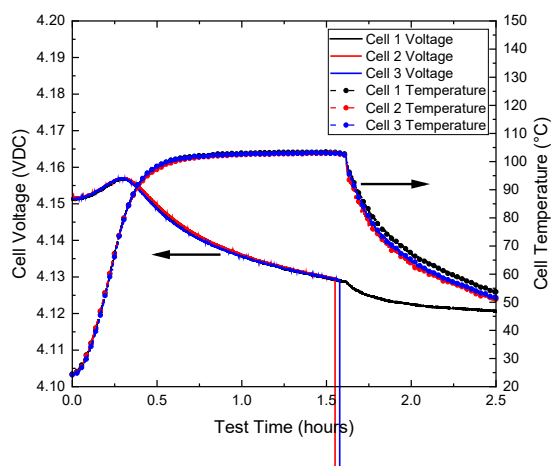


Figure 1. Open circuit voltage (OCV) and skin temperature of 100% SOC cells exposed to 100 °C thermal insult for 100 minutes.

Irreversible capacity loss after the thermal insult was found to correlate most strongly with exposure duration, as shown in **Figure 2**. Observed irreversible capacity loss was generally very mild and on the order of a few percent of the originally measured capacity, with the exception of cells where CID activation was observed and prevented charge and discharge cycling to measure capacity. Temperature was also seen to have a mild effect, with capacity loss generally increasing with temperature. For cells exposed to 90 °C and 100 °C for 100 minutes, increasing SOC from 30% to 100% slightly increased irreversible capacity loss and led to CID activation for some of the cells exposed at 100% SOC.

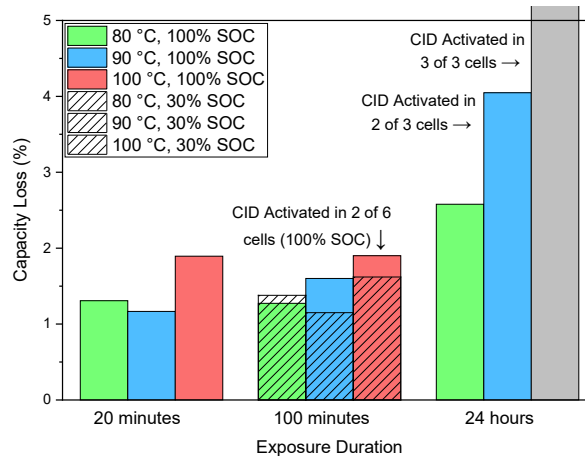


Figure 2. Irreversible capacity loss after thermal insult measured as average C/5 capacity before and after thermal insult.

Representative Nyquist plots displaying real (Z_{re}) and imaginary (Z_{im}) components of AC impedance measured by EIS (**Figure 3**) show the characteristic depressed semi-circle and semi-infinite diffusion tail expected for lithium-ion batteries. Milder thermal insult conditions, notably those with only 20-minute durations or an exposure temperature of 80 °C, resulted in a decrease in total electrochemical impedance based on the low-frequency intercept of the Nyquist plot.

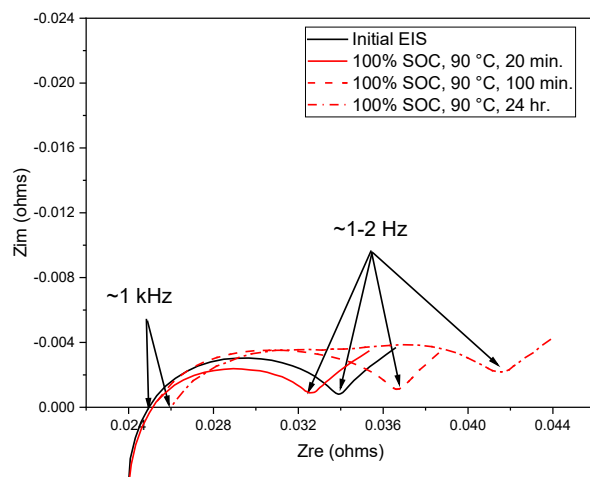


Figure 3. Nyquist plots displaying representative AC impedance for cells before and after thermal insult, collected at 30% SOC and 25 °C.

A summary of AC impedance changes after thermal insult is shown **Figure 4** and followed a similar trend to irreversible capacity loss, with the greatest changes observed for 24-hour exposure durations. The starting AC impedance of the cells used in this study was approximately $35 \pm 1 \text{ m}\Omega$, meaning the observed increase in impedance was on the order of $6 \text{ m}\Omega$.

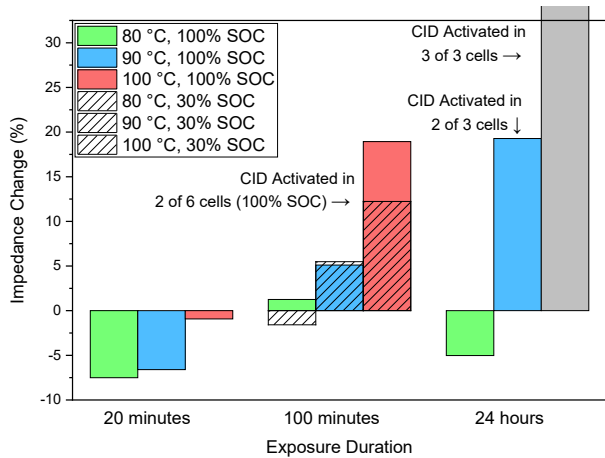


Figure 4. AC impedance change after thermal insult measured at 30% SOC and 25 °C.

Differential capacity plots were derived from C/5 cycling data to observe changes in the electrochemical behavior of cells before and after the thermal insult experiment. As shown in **Figure 5**, slight changes in the four main peaks observed during cell charging are seen, with the magnitude of these shifts increasing at the highest temperatures and longest duration exposures. Like with impedance and capacity measurements, evaluation of cells subjected to 100 °C for 24 hours was not possible due to CID activation.

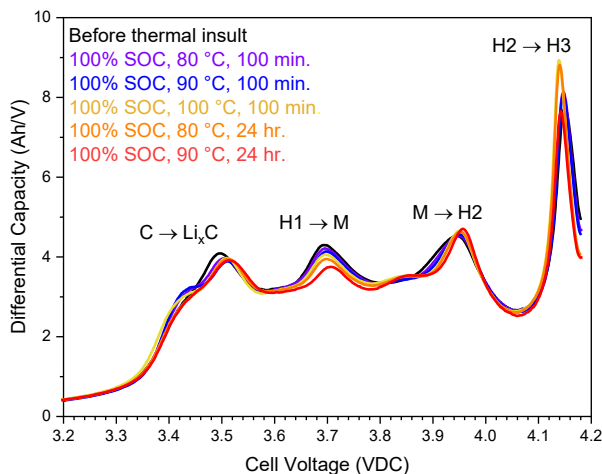


Figure 5. Differential capacity (dQ/dV) vs. voltage for cells before and after thermal insult.

The observed peaks are assigned to structural changes in the graphite/Si anode and NCM811 cathode, specifically the lithiation of graphite to form Li_xC occurring at $\sim 3.5\text{V}$, followed by crystallographic unit cell transformations in the NCM811 cathode assigned to hexagonal to monoclinic ($\text{H1} \rightarrow \text{M}$), monoclinic to hexagonal ($\text{M} \rightarrow \text{H2}$), and hexagonal to hexagonal ($\text{H2} \rightarrow \text{H3}$) transformations, occurring at $\sim 3.7\text{V}$, $\sim 3.95\text{V}$, and $\sim 4.15\text{V}$, respectively [8]. Analogous peaks are also observed during discharge but are not shown in Figure 5 for clarity. Shifting of the dQ/dV

peaks indicates irreversible structural damage occurring in both the anode and cathode materials, with decreasing peak intensity correlating to a loss in electrochemically active electrode materials and shifting peak potentials to higher potentials on charge indicating an increased electrochemical overpotential. The formation of new low-intensity peaks, notably occurring between the $\text{H1} \rightarrow \text{M}$ and $\text{M} \rightarrow \text{H2}$ cathode active material structural transitions also suggests that new electrochemically active phases have been produced.

Heat flow of cells before and after thermal insult is shown in **Figure 6** during a C/5 charge and discharge cycle starting from 0% SOC. Heat flow is seen to vary as a function of SOC, and the general appearance of the heat flow during charge and discharge are different despite the use of an identical current. A slight shift along the X-axis (test time in hours) is observed for cells exposed to the most abusive thermal insult conditions, which is related to the lower capacity of these cells due to the irreversible capacity loss described in Figure 2. Total heat produced for all cells was comparable and was approximately 330 mJ during charge and 250 mJ during discharge regardless of thermal insult condition.

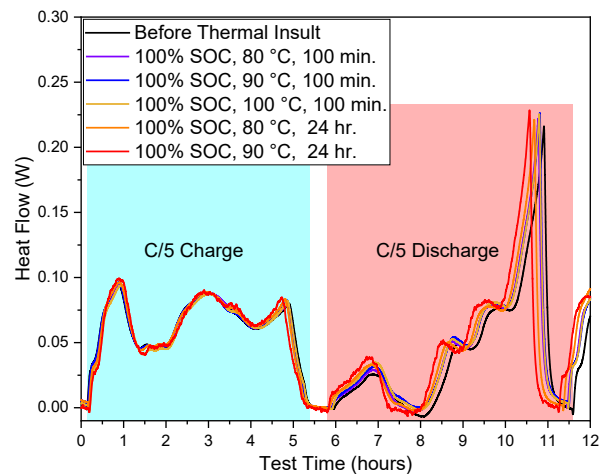


Figure 6. Heat flow during C/5 (680 mA) charge and discharge cycle for cells before and after thermal insult.

Accelerating rate calorimetry testing was conducted on as received and post thermal insult cells to evaluate changes in thermal runaway behavior. As seen in **Figure 7**, the onset of rapid-self heating and maximum self-heating rate for all cells was similar. Critical temperatures associated with the onset of exothermic reactions (defined as the temperature at which a self-heating rate of $>0.02\text{ °C/min}$ was first observed), venting (observed as a negative heating rate and slight temperature drop), thermal runaway (defined as the temperature at which self-heating exceeds 5 °C/min), and maximum temperature are shown in **Table 1**. Mass loss expressed as a percentage of the original cell mass is also provided.

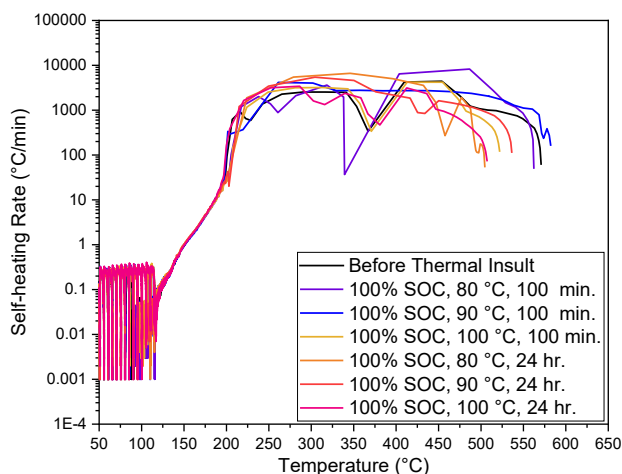


Figure 7. Self-heating rate vs. temperature for Accelerating Rate Calorimetry (ARC) testing of cells before and after thermal insult.

Table 1. Critical temperatures and mass loss observed during Accelerating Rate Calorimetry (ARC) experiments before and after thermal insult.

Cell	T _{Exo} (°C)	T _{vent} (°C)	T _{TR} (°C)	T _{MAX} (°C)	Δ mass
Before Thermal Insult	88	112	177	585	-74%
100%SOC 80 °C 100 min.	91	108	177	618	-76%
100%SOC 90 °C 100 min.	93	111	175	614	-72%
100%SOC 100 °C 100 min.	94	110	178	535	-76%
100%SOC 80 °C 24 hr.	96	109	176	505	-71%
100%SOC 90 °C 24 hr.	106	112	176	494	-77%
100%SOC 100 °C 24 hr.	110	110	177	522	-73%

As seen in Figure 7, temperatures recorded for the onset of thermal runaway (T_{TR}) are very similar, as were temperatures recorded for cell venting (T_{vent}), maximum temperature (T_{MAX}), and mass loss. However, the onset of exothermic reactions (T_{EXO}) was observed to increase with increasing temperature and duration of the thermal abuse experiment. This behavior is interpreted as evidence that the thermal insult experiments exceeded the threshold to begin these same exothermic reactions, however as shown in all

the data collected, this did not lead to a significant lasting impact on cell performance and safety.

Conclusions

Commercially available high-energy 18650 lithium-ion cells were subjected to temperatures exceeding the onset of exothermic behavior. In some cases, CID activation led to an “open circuit” failure state which prevented further analysis, however for all surviving cells only mild capacity loss and impedance rise were observed. Measurements of heat flow and thermal stability by IBC and ARC also indicate that these cells are robust to the “thermal insult” conditions explored in this study.

Acknowledgements

Funding for this effort was provided by NAVSEA.

References

- [1] D. Ren, H. Hsu, R. Li, X. Feng, D. Guo, X. Han, L. Lu, X. He, S. Gao, J. Hou, Y. Li, Y. Wang and M. Ouyang, "A comparative investigation of aging effects on thermal runaway behavior of lithium-ion batteries," *eTransportation*, no. 100034, 2019.
- [2] D. Doughty and P. Roth, "Thermal runaway caused fire and explosion of lithium ion battery," *The Electrochemical Society Interface*, 2012.
- [3] T. Bandhauer, S. Garimella and T. Fuller, "A Critical Review of Thermal Issues in Lithium-ion Batteries," *Journal of The Electrochemical Society*, vol. 158, no. 3, pp. R1-R25, 2011.
- [4] Q. Wang, P. Ping, X. Zhao, G. Chu, J. Sun and C. Chen, "Thermal runaway caused fire and explosion of lithium ion battery," *Journal of Power Sources*, vol. 208, pp. 210-224, 2012.
- [5] Y. Preger, L. Torres-Castro, T. Rauhala and J. Jeevarajan, "Perspective—On the Safety of Aged Lithium-Ion Batteries," *Journal of the Electrochemical Society*, vol. 169, no. 030507, 2022.
- [6] C. Geisbauer, K. Wohrl, C. Mittman and H. Schweiger, "Review—Review of Safety Aspects of Calendar Aged Lithium Ion Batteries," *Journal of the Electrochemical Society*, vol. 167, no. 090523, 2020.
- [7] N. Spinner, K. Hinnant, R. Mazurick, A. Brandon, S. Rose-Pehrson and S. Tuttle, "Novel 18650 lithium-ion battery surrogate cell design with anisotropic thermophysical properties for studying failure events," *Journal of Power Sources*, vol. 312, pp. 1-11, 2016.
- [8] P. West, C. Quilty, Z. Wang, S. Ehrlich, L. J. C. Ma, D. Fischer, X. K. A. Tong, E. Takeuchi, A. Marschlok, K. Takeuchi and D. Bock, "Degradation in Ni-Rich LiNi_{1-x-y}Mn_xCoyO₂/Graphite Batteries: Impact of Charge Voltage and Ni Content," *Journal of Physical Chemistry C*, vol. 127, no. 15, pp. 7054-7070, 2023.